

## 2 Seismic Sources: stress glut, moment tensor and beach balls

---



*Shakemovie* snapshot with a beachball representation of a CMT solution for a Mw 6.9 earthquake off the coast in Northern California, 2014.

### Introduction

We introduce earthquakes as a failure of Hooke's law. Furthermore we simplify the displacement on a fault and the extent of the rupture. These approximations of ideal faults and point sources then become important to describe earthquakes using moment tensor solutions which can be represented as beachballs. For large earthquakes, kinematic and dynamic rupture solutions are presented. We also define the moment magnitude of an earthquake and give a brief overview over statistical behaviour of earthquake sources. At the end, we mention more exotic types of sources which cause ground shaking and are commonly investigated in research projects.

### Learn objectives

- You know what stress glut is.
- You know what a moment tensor is.
- You are able to explain a beachball representation.
- You know the difference between dynamic and kinematic rupture solutions.
- You are familiar with power laws occurring in earthquake seismology.

## 2.1 Indigenous sources as localized failure

### It's all Hooke's fault

Let  $\mathbf{u}$  be a continuous displacement vector in an everywhere solid Earth model  $\oplus$  bounded by  $\partial\oplus$  and characterized by density  $\rho$  and elastic tensor  $\mathbf{c}$ . The linearized momentum equation governing the deformation in  $\oplus$  reads

$$\rho \partial_t^2 \mathbf{u} = \nabla \cdot \boldsymbol{\tau} \text{ in } \oplus \quad (2.1)$$

subject to the *constitutive elastic stress-strain relationship* (“Hooke’s Law”)

$$\boldsymbol{\tau} = \mathbf{c} : \nabla \mathbf{u} \text{ in } \oplus, \quad (2.2)$$

and the dynamical free-surface boundary condition

$$\hat{\mathbf{n}} \cdot \boldsymbol{\tau} = \mathbf{0} \text{ on } \partial\oplus. \quad (2.3)$$

**Theorem.** There are no earthquakes; we have eternal seismic quiescence in  $\oplus$ .

**Proof:**  $\mathbf{u}(\mathbf{x}, t) = \mathbf{0}$  is the unique solution to eqs (2.1)–(2.3) for initial conditions  $\mathbf{u}(\mathbf{x}, 0) = \mathbf{0}$  and  $\partial_t \mathbf{u}(\mathbf{x}, 0) = \mathbf{0}$ .

.....Hoo? What on earth? No quakes?

Something must be wrong from the outset eqs (2.1)–(2.3). Eqs (2.1) and (2.3) result from *Newton’s Laws*, so Hooke’s “Law” must break down.

**Note:** *Constitutive relationships* are **not** laws! They merely describe an assumed, empirical behavior of an idealized material subjected to a force. In other words:

*An earthquake is a localized transient failure of Hooke’s “Law”.*

**Definition.** An *indigenous source* is any phenomenon occurring entirely within or upon the surface of  $\oplus$  that does not involve forces exerted by any other bodies. Examples: Slip on a fault, sudden phase change. Meteorite impacts are **not** indigenous sources.

### Stress glut & equivalent forces

We now introduce modifications to the stress-strain relationship to describe this failure with model (Hooke) stress  $\boldsymbol{\tau}^{\text{model}}$ , and true stress  $\boldsymbol{\tau}^{\text{true}}$  such that  $\boldsymbol{\tau}^{\text{model}} = \mathbf{c} : \nabla \mathbf{u}$ , and  $\rho \partial_t^2 \mathbf{u} = \nabla \cdot \boldsymbol{\tau}^{\text{true}}$ , and

$$\rho \partial_t^2 \mathbf{u} - \nabla \cdot \boldsymbol{\tau}^{\text{model}} = -\nabla \cdot (\boldsymbol{\tau}^{\text{model}} - \boldsymbol{\tau}^{\text{true}}) \text{ in } \oplus, \quad (2.4)$$

$$\hat{\mathbf{n}} \cdot \boldsymbol{\tau}^{\text{model}} = \hat{\mathbf{n}} \cdot (\boldsymbol{\tau}^{\text{model}} - \boldsymbol{\tau}^{\text{true}}) \text{ on } \partial\oplus. \quad (2.5)$$

Defining  $\mathbf{S} = \boldsymbol{\tau}^{\text{model}} - \boldsymbol{\tau}^{\text{true}}$  as the *stress glut*, and writing  $\boldsymbol{\tau}$  instead of  $\boldsymbol{\tau}^{\text{model}}$  for brevity, we obtain

$$\rho \partial_t^2 \mathbf{u} - \nabla \cdot \boldsymbol{\tau} = \mathbf{f} \text{ in } \oplus, \quad (2.6)$$

$$\boldsymbol{\tau} = \mathbf{c} : \nabla \mathbf{u} \text{ in } \oplus, \quad (2.7)$$

$$\hat{\mathbf{n}} \cdot \boldsymbol{\tau} = \mathbf{t} \text{ on } \partial\oplus, \quad (2.8)$$

subject to initial conditions  $\mathbf{u}(\mathbf{x}, 0) = \mathbf{0}$ ,  $\partial_t \mathbf{u}(\mathbf{x}, 0) = \mathbf{0}$ . The right hand sides of eqs (2.6) and (2.8) are the equivalent body force  $\mathbf{f} = -\nabla \cdot \mathbf{S}$  (non-zero in  $\Sigma$ ), and equivalent surface force  $\mathbf{t} = \hat{\mathbf{n}} \cdot \mathbf{S}$  (non-zero on  $\partial\Sigma \cap \partial\oplus$ ), where  $\Sigma$  is the volume of the earthquake fault. The stress glut vanishes everywhere outside of the instantaneous failure region  $\Sigma$ , including on its buried boundary:

$$\mathbf{S} = \mathbf{0} \text{ in } \oplus - \Sigma \text{ and on } \partial\Sigma - \partial\Sigma \cap \partial\oplus. \quad (2.9)$$

Note that slip may extend to the free surface such that  $\mathbf{S}$  would be non-zero in  $\partial\Sigma \cap \partial\oplus$ . Defined as the difference between two symmetric stress tensors, the *stress glut* tensor is also symmetric:  $\mathbf{S} = \mathbf{S}^T$ .

The total force exerted on  $\oplus$  is given by

$$\mathcal{F}_{\text{tot}} = \int_{\oplus} \mathbf{f} d^3\mathbf{x} + \int_{\partial\oplus} \mathbf{t} d^2\mathbf{x} = - \int_{\Sigma} \nabla \cdot \mathbf{S} d^3\mathbf{x} + \int_{\partial\Sigma \cap \partial\oplus} \hat{\mathbf{n}} \cdot \mathbf{S} d^2\mathbf{x} = \int_{\partial\Sigma - \partial\Sigma \cap \partial\oplus} \hat{\mathbf{n}} \cdot \mathbf{S} d^2\mathbf{x} = \mathbf{0}, \quad (2.10)$$

where we have limited integration to  $\Sigma$  by the localized nature of  $\mathbf{f}$  and utilized Gauss' Theorem. The total torque  $\mathcal{N} = \int_{\oplus} (\mathbf{x} \times \mathbf{f}) d^3\mathbf{x} + \int_{\partial\oplus} (\mathbf{x} \times \mathbf{t}) d^2\mathbf{x}$  becomes

$$\mathcal{N}_i^{\text{tot}} = - \int_{\Sigma} \epsilon_{ijk} x_j \partial_l S_{lk} d^3\mathbf{x} + \int_{\partial\Sigma \cap \partial\oplus} \epsilon_{ijk} x_j n_l \partial_l S_{lk} d^2\mathbf{x} = \int_V \epsilon_{ilk} S_{lk} d^3\mathbf{x} - \int_{\partial\Sigma \cap \partial\oplus} \epsilon_{ijk} x_j n_l S_{lk} d^2\mathbf{x} = 0, \quad (2.11)$$

thus vanishes.

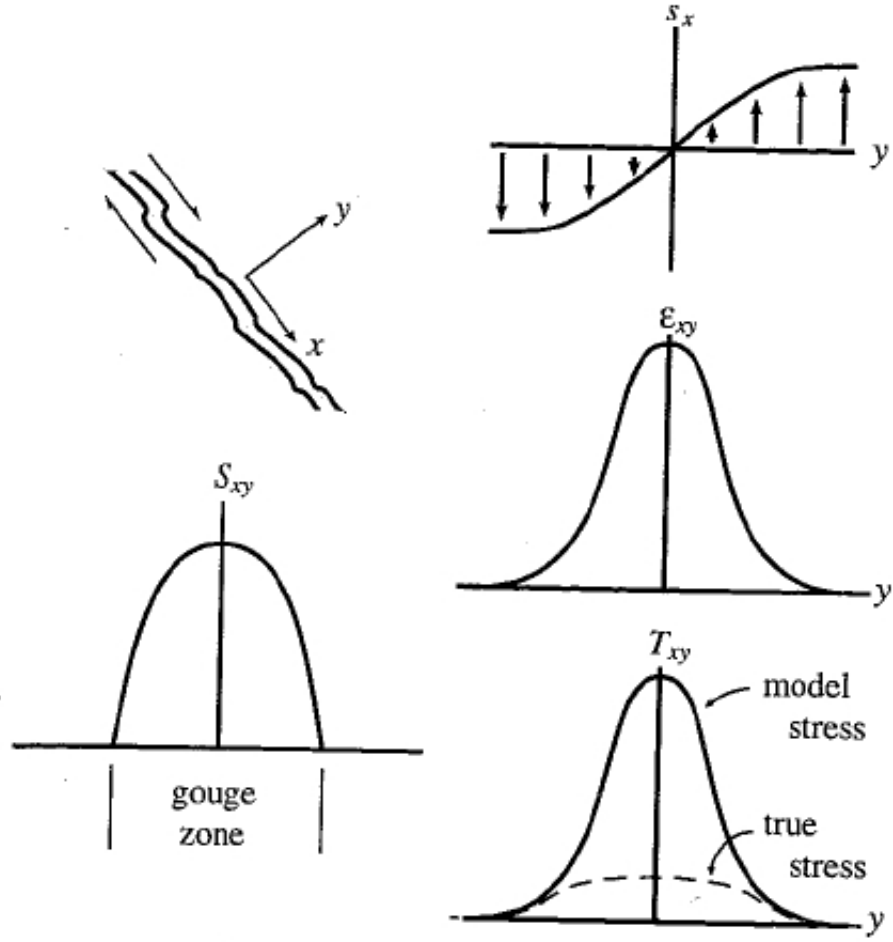


Figure 1: *Schematic map view of a right-lateral vertical strike-slip fault, showing the horizontal coordinates  $x$  and  $y$ . Shading depicts the idealized gouge zone within which Hooke's law fails. Top right: Displacement  $s_x$  versus perpendicular distance  $y$  within the gouge zone. Middle right: Corresponding shear strain  $\epsilon_{xy}$ . Bottom right: Model and shear stresses  $\tau_{xy}$ . Bottom left: The stress glut  $S_{xy} = \tau_{xy}^{\text{model}} - \tau_{xy}^{\text{true}}$  is zero outside of the gouge zone.*

### Mathematical excursion: Distribution theory

**Definition.** A *distribution*  $f$  is a continuous, linear functional on a space of smooth test functions  $\phi$  defined in  $\oplus$  and  $\phi = 0$  on  $\partial\oplus$ :  $f : \langle f, \phi \rangle \rightarrow \text{scalar}$ , often written as  $\langle f, \phi \rangle = \int_{\oplus} f \phi d^3\mathbf{x}$ , where the integral represents a symbolic operation since distributions are not generally integrable.

Some observations & properties:

- Any ordinary function  $f$  can be thought of as a distribution (“*regular distributions*”).
- Write  $\mathcal{D}f$  when thinking of function  $f$  as a distribution.
- Example: Dirac delta distribution:  $\langle \delta_0, \phi \rangle = \phi(x_0)$  (“*singular distribution*”), such that  $\int_{\oplus} \delta_0 \phi d^3\mathbf{x} = \int_{\oplus} \delta(\mathbf{x} - \mathbf{x}_0) \phi(\mathbf{x}) d^3\mathbf{x} = \phi(\mathbf{x}_0)$ .
- If  $f$  is an ordinary function, then  $\int_{\oplus} \nabla f \phi d^3\mathbf{x} = - \int_{\oplus} f \nabla \phi d^3\mathbf{x}$ .

Weighted distribution  $\langle w \delta_{\Sigma}, \phi \rangle = \int_{\Sigma} w \phi d^2\mathbf{x}$ , and  $w \delta_{\Sigma} = \int_{\Sigma} w(\boldsymbol{\xi}) \delta(\mathbf{x} - \boldsymbol{\xi}) d^2\boldsymbol{\xi}$ . Then

$$\langle w \delta_{\Sigma}, \phi \rangle = \int_{\oplus} \int_{\Sigma} w(\boldsymbol{\xi}) \delta(\mathbf{x} - \boldsymbol{\xi}) \phi(\mathbf{x}) d^2\boldsymbol{\xi} d^3\mathbf{x} = \int_{\Sigma} w(\boldsymbol{\xi}) \phi(\boldsymbol{\xi}) d^2\boldsymbol{\xi}$$

Another example: Function  $f$  is smooth everywhere in  $\oplus$  except on  $\Sigma$  where it has a discontinuity  $[f]_{-}^{+}$ . What is  $\nabla f$ ? Non-existent.....instead: What is  $\nabla(\mathcal{D}f)$ ?  $\langle \nabla(\mathcal{D}f), \phi \rangle = - \lim_{\epsilon \rightarrow 0} \int_{\oplus - \oplus_{\epsilon}} f \nabla \phi d^3\mathbf{x}$ . Undo partial integration, execute  $\epsilon \rightarrow 0$ :

$$\lim_{\epsilon \rightarrow 0} \left[ - \int_{\partial\oplus_{\epsilon}} \hat{\mathbf{n}} f \phi d^2\mathbf{x} + \int_{\oplus - \oplus_{\epsilon}} \nabla f \phi d^3\mathbf{x} \right] = \int_{\Sigma} \hat{\nu} [f]_{-}^{+} \phi d^2\mathbf{x} + \int_{\oplus} \nabla f \phi d^3\mathbf{x}, \quad (2.12)$$

such that we arrive at

$$\nabla(\mathcal{D}f) = \mathcal{D}(\nabla f) + \hat{\nu} [f]_{-}^{+} \delta_{\Sigma}. \quad (2.13)$$

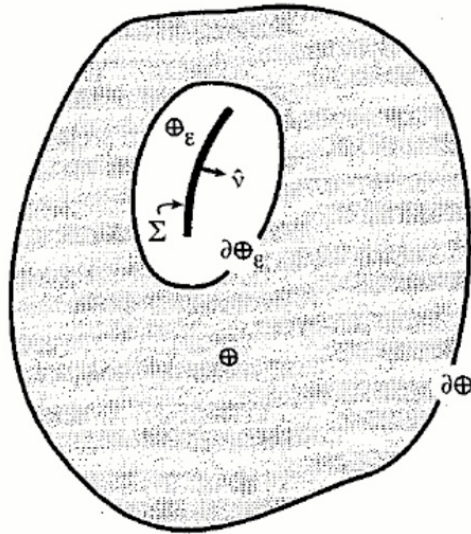


Figure 2: In gray: The integration volume for eq. (2.12). In the limit  $\epsilon \rightarrow 0$  the interior boundary  $\partial\oplus_{\epsilon}$  collapses onto the embedded discontinuity surface  $\Sigma$ .

## Ideal faults

**Definition.** An *ideal fault* is an infinitesimally thin surface  $\Sigma$  embedded within  $\oplus$ , across which there is a tangential slip discontinuity  $\Delta \mathbf{u} = [\mathbf{u}]_{-}^{+}$ . The walls of the fault obey  $\hat{\nu} \cdot \Delta \mathbf{u} = 0$  on  $\Sigma$ , i.e. cannot separate or interpenetrate. Slip  $\Delta \mathbf{u}$  must vanish on the instantaneous edge  $\partial \Sigma$  of the fault, except when intersecting a solid surface or seafloor.

The true stress  $\boldsymbol{\tau}^{\text{true}}$  is discontinuous across  $\Sigma$ , but the associated distribution  $\mathcal{D}(\boldsymbol{\tau}^{\text{true}})$  is regular:  $\mathcal{D}(\boldsymbol{\tau}^{\text{true}}) = \mathbf{c} : \mathcal{D}(\nabla \mathbf{u})$ . The model stress is a singular distribution:  $\boldsymbol{\tau}^{\text{model}} = \mathbf{c} : \nabla(\mathcal{D}\mathbf{u})$ . Using the distribution derivative relation, the stress glut becomes

$$\mathbf{S} = \boldsymbol{\tau}^{\text{model}} - \boldsymbol{\tau}^{\text{true}} = \mathbf{c} : [\nabla(\mathcal{D}\mathbf{u}) - \mathcal{D}(\nabla \mathbf{u})] = (\mathbf{c} : \hat{\nu} \Delta \mathbf{u}) \delta_{\Sigma}. \quad (2.14)$$

It is convenient to define the stress-glut density on  $\Sigma$  by  $\mathbf{m} = \mathbf{c} : \hat{\nu} \Delta \mathbf{u}$  or  $m_{ij} = c_{ijkl} \nu_k \Delta u_l$ , such that  $\mathbf{S} = \mathbf{m} \delta_{\Sigma}$ , which is also known as the *surface moment-density tensor* and describes the stress glut per unit area on each infinitesimal patch of the fault. The stress glut is a singular distribution across an ideal fault: Identical to zero everywhere except on  $\Sigma$ . Since the product of a discontinuous function and a Dirac delta distribution is not defined, one stipulates that  $\mathbf{c}$  is continuous across the fault surface:  $[\mathbf{c}]_{-}^{+} = \mathbf{0}$  on  $\Sigma$ . We can now write the equivalent body and surface force densities respectively as

$$\mathbf{f} = -\mathbf{m} \cdot \nabla \delta_{\Sigma} \text{ in } \oplus; \quad \mathbf{t} = (\hat{\mathbf{n}} \cdot \mathbf{m}) \delta_{\Sigma} \text{ on } \partial \oplus. \quad (2.15)$$

$\mathbf{f}$  vanishes everywhere except on the instantaneous fault surface  $\Sigma$ , and  $\mathbf{t}$  everywhere except upon the surface rupture trace  $\partial \Sigma \cap \partial \oplus$ . Eqs (2.15) encapsulate *time-dependent faulting in anisotropic Earth models for arbitrary fault geometry*. The net torque vanishes by virtue of the symmetry  $\mathbf{m}^T = \mathbf{m}$ . This symmetry can be written in diagonal form as

$$\mathbf{m} = m_{+} \hat{\mathbf{e}}_{+} \hat{\mathbf{e}}_{+} + m_0 \hat{\mathbf{e}}_0 \hat{\mathbf{e}}_0 + m_{-} \hat{\mathbf{e}}_{-} \hat{\mathbf{e}}_{-} \quad (2.16)$$

where  $m_{+} \geq m_0 \geq m_{-}$  are the eigenvalues and  $\hat{\mathbf{e}}_{+}, \hat{\mathbf{e}}_{-}, \hat{\mathbf{e}}_0$  are the normalized eigenvectors. Thus,  $\mathbf{f}$  can be interpreted as a distribution of mutually perpendicular linear vector dipoles. In an isotropic Earth with hydrostatic initial stress ( $\kappa$ : incompressibility,  $\mu$ : rigidity) we can simplify  $c_{ijkl} = (\kappa - 2/3\mu)\delta_{ij}\delta_{kl} + \mu(\delta_{ik}\delta_{jl} + \delta_{il}\delta_{jk})$ . Diagonal terms  $\delta_{ij}\delta_{kl}$  cannot contribute since this would represent a volumetric change or fault opening. Thus, we get

$$\mathbf{m} = \mu \Delta u (\hat{\mathbf{e}}_{+} \hat{\mathbf{e}}_{+} - \hat{\mathbf{e}}_{-} \hat{\mathbf{e}}_{-}) = \mu \Delta u (\hat{\nu} \hat{\boldsymbol{\sigma}} + \hat{\boldsymbol{\sigma}} \hat{\nu}), \quad (2.17)$$

where  $\hat{\mathbf{e}}_{\pm} = \frac{1}{\sqrt{2}}(\hat{\nu} \pm \hat{\boldsymbol{\sigma}})$ , and  $\Delta u$  is the magnitude of the slip vector and  $\hat{\boldsymbol{\sigma}}$  is the slip direction:  $\Delta \mathbf{u} = \Delta u \hat{\boldsymbol{\sigma}}$ . The equivalent body force  $\mathbf{f}$  may be regarded as a distribution of *double couples* on  $\Sigma$ , as the derivative of  $\delta_{\Sigma}$  contains both positive and negative components.

These results have been obtained independently by Burridge and Knopoff (1964) albeit using a more cumbersome derivation, and the double-couple concept represents one of the

cornerstones in assessing earthquake sources.

## 2.2 Point-source approximation

Earthquakes can be approximated as originating from point  $\mathbf{x}_s$  (“*hypocenter*”) under these assumptions:

- long wavelengths, much larger than source/rupture dimensions,
- long seismic periods, much larger than source/rupture duration.

### The moment tensor

The strain eigenfunctions in the mode summation (using normal modes) can be expanded in a Taylor series; only keeping the zero-th order term, we obtain

$$\boldsymbol{\epsilon}_k(\mathbf{x}) \begin{Bmatrix} \cos \omega_k t \\ \sin \omega_k t \end{Bmatrix} \approx \boldsymbol{\epsilon}_k(\mathbf{x}_s) \begin{Bmatrix} \cos \omega_k t_s \\ \sin \omega_k t_s \end{Bmatrix}, \quad (2.18)$$

where  $t_s$  is the origin time. Thus, e.g.,

$$a_k \approx \mathbf{M} : \boldsymbol{\epsilon}_k(\mathbf{x}_s) \cos \omega_k t_s, \text{ where} \quad (2.19)$$

$$\mathbf{M} = \int_{t_0}^{t_f} \int_{\Sigma} \partial_t \mathbf{S} d^3 \mathbf{x} dt = \int_{\Sigma} \mathbf{S}^{\text{final}} d^3 \mathbf{x}. \quad (2.20)$$

$\mathbf{M} = \mathbf{M}^T$  is the (symmetric) *moment tensor*, containing 6 independent components, and  $\mathbf{S}^{\text{final}}$  is the final static stress. Slip on a fault can then be expressed via

$$\mathbf{M} = \int_{\Sigma} \mathbf{m}^{\text{final}} d^2 \boldsymbol{\xi}, \quad (2.21)$$

and the moment tensor in an isotropic Earth model becomes

$$\mathbf{M} = \int_{\Sigma} \mu \Delta u^{\text{final}} (\hat{\boldsymbol{\nu}} \hat{\boldsymbol{\sigma}} + \hat{\boldsymbol{\sigma}} \hat{\boldsymbol{\nu}}) d^2 \mathbf{x}. \quad (2.22)$$

The glut rate is  $\partial_t \mathbf{S} = \mathbf{M} \delta(\mathbf{x} - \mathbf{x}_s) \delta(t - t_s)$ , and the equivalent body force becomes

$$\mathbf{f} = -\mathbf{M} \cdot \nabla_{\mathbf{x}} \delta(\mathbf{x} - \mathbf{x}_s) H(t - t_s). \quad (2.23)$$

For a uni-directional slip on a planar fault,  $\hat{\boldsymbol{\nu}}, \hat{\boldsymbol{\sigma}}$  are constant such that  $\mathbf{M} = M_0 (\hat{\boldsymbol{\nu}} \hat{\boldsymbol{\sigma}} + \hat{\boldsymbol{\sigma}} \hat{\boldsymbol{\nu}})$ , where

$$M_0 = \int_{\Sigma} \mu \Delta u^{\text{final}} d^2 \mathbf{x} \quad (2.24)$$

is called the *scalar moment* (Aki 1966), and has been the standard measure of the size of an earthquake. More generally, the scalar moment of an arbitrary moment tensor can be defined by

$$M_0 = \frac{1}{\sqrt{2}} (\mathbf{M} : \mathbf{M})^{1/2}. \quad (2.25)$$

Taking the next term in the Taylor expansion of  $\epsilon_k^*(\mathbf{x}) \{\cos \omega_k t\}$  in eq (2.18) into account, one can develop an improved approximation, leading to the *centroid moment tensor (CMT)* ([globalcmt.org](http://globalcmt.org)), which now forms the basis for determining earthquake parameters (Details: Dahlen & Tromp, 5.4.2).

**Figure 4.4-4: Nine force couples which compose the seismic moment tensor.**

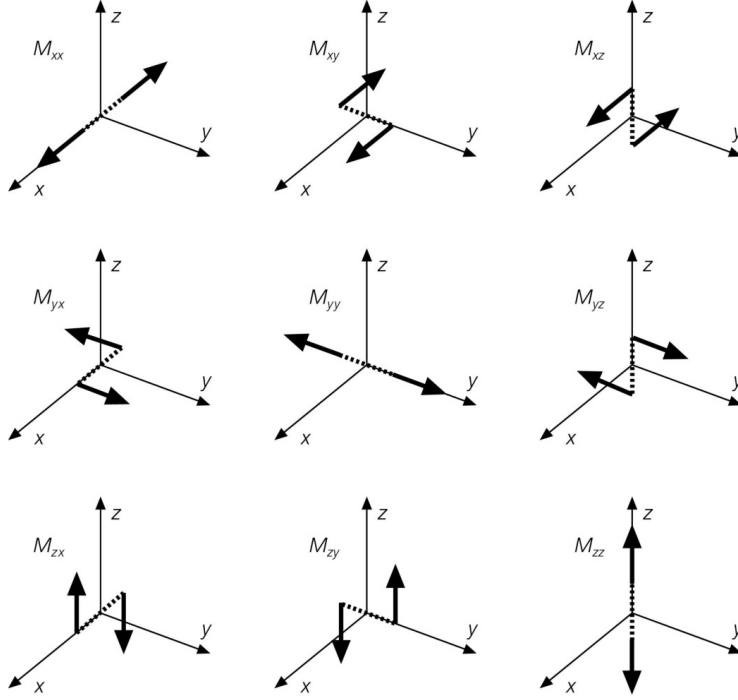


Figure 3: The respective force couples of each element of the moment tensor. The symmetry of the tensor means that for instance  $M_{xy}$  represents the same radiation as  $M_{yx}$ , i.e. fault and auxiliary planes are indistinguishable (see “Fault classification”).

### Radiation patterns & beach balls

Symmetric moment tensors can be decomposed into their isotropic and deviatoric parts as

$$\mathbf{M} = \frac{1}{3} \text{tr}(\mathbf{M})\mathbf{I} + \mathbf{M}^{\text{dev}}. \quad (2.26)$$

An ideal fault in an isotropic Earth with hydrostatic stress has no isotropic part, i.e.  $\text{tr}(\mathbf{M}) = 0$ , which is generally the case in virtually all studies on earthquakes, and an assumption in calculation CMT solutions (“linear constraint”).  $\mathbf{M}^{\text{dev}}$  will be a double-couple if  $\det \mathbf{M}^{\text{dev}} = 0$  (“non-linear constraint”).

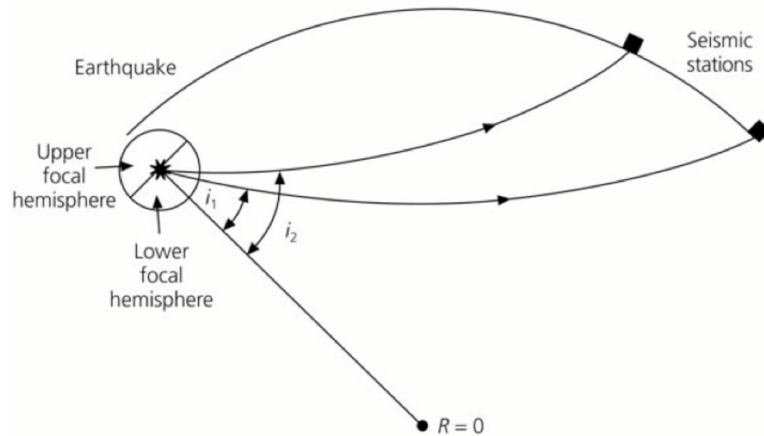


Figure 4: Focal mechanism and hemisphere.  $i$ : angle of incidence (take-off angle), i.e. angle at which the ray intersects the focal hemisphere.



**Beach Balls:**  $P$ -wave amplitudes on a focal sphere are given by  $\hat{\mathbf{r}} \cdot \mathbf{M} \cdot \hat{\mathbf{r}}$ . Beach balls are a common way to plot the radiation patterns, separating amplitudes into positive and negative fractions as a function of azimuth. One plots  $\gamma_i M_{ij} \gamma_j = \hat{\mathbf{r}} \cdot \mathbf{M} \cdot \hat{\mathbf{r}}$  on the *lower focal hemisphere* where  $\gamma_i$  are the direction cosines, and views the stereographic projection from above. Black means  $\hat{\mathbf{r}} \cdot \mathbf{M} \cdot \hat{\mathbf{r}} > 0$ , white negative.

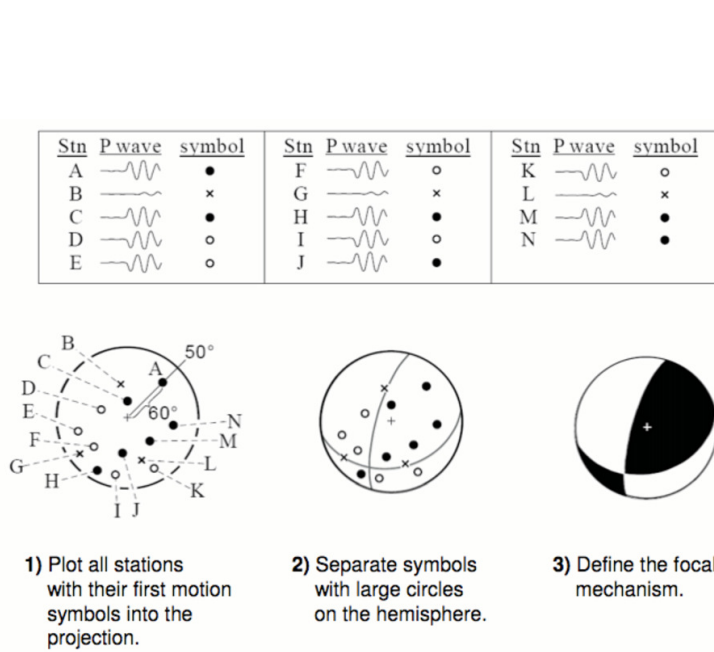


Figure 5: First  $P$ -wave motions, focal mechanism and the graphic determination of beach balls.

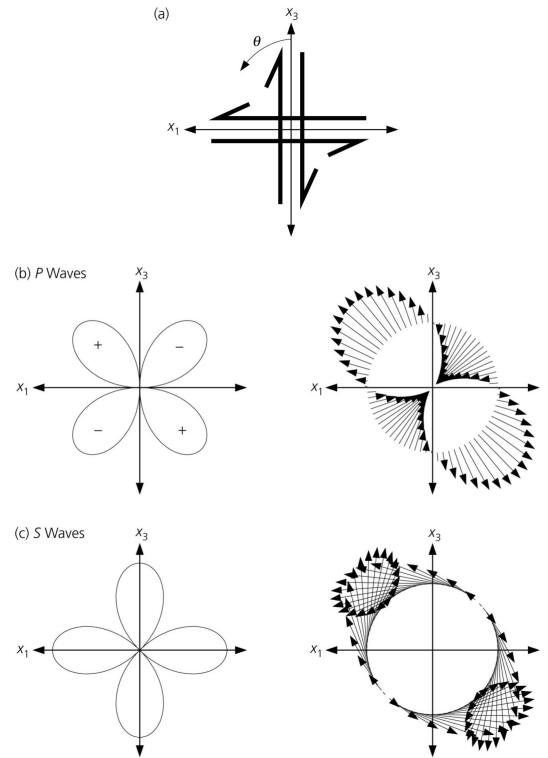


Figure 6:  $P$  and  $S$  amplitude radiation patterns for a double-couple source.

First motions on seismograms cannot distinguish which nodal plane (fault plane or auxiliary plane) is actually the fault due to the double-couple ambiguity in radiation. Oftentimes, independent data is utilized to constrain the fault, e.g. geological or geodetic measurements, or aftershocks along the fault. If the point-source approximation fails, finite time to slip across the fault can also be used to infer the fault plane.

### Some observations:

- all radiation patterns include the same seismic moment  $\rightarrow$  vertical strike-slip produces much stronger Love waves than a vertical dip-slip.
- Most modern source studies are based on *waveform modeling* instead of first motion.
- Surface waves provide information about depths, as excitation functions depend on depth.
- Strong *directivity effect* caused by surface waves.

- A combination of body and surface waves is often useful to constrain both nodal planes.


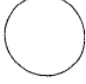










Moment Tensor	Beachball	Moment Tensor	Beachball
$\frac{1}{\sqrt{3}} \begin{pmatrix} 1 & 0 & 0 \\ 0 & 1 & 0 \\ 0 & 0 & 1 \end{pmatrix}$		$-\frac{1}{\sqrt{3}} \begin{pmatrix} 1 & 0 & 0 \\ 0 & 1 & 0 \\ 0 & 0 & 1 \end{pmatrix}$	
$-\frac{1}{\sqrt{2}} \begin{pmatrix} 0 & 0 & 0 \\ 0 & 0 & 1 \\ 0 & 1 & 0 \end{pmatrix}$		$\frac{1}{\sqrt{2}} \begin{pmatrix} 0 & 0 & 0 \\ 0 & 1 & 0 \\ 0 & 0 & -1 \end{pmatrix}$	
$\frac{1}{\sqrt{2}} \begin{pmatrix} 0 & 1 & 0 \\ 1 & 0 & 0 \\ 0 & 0 & 0 \end{pmatrix}$		$\frac{1}{\sqrt{2}} \begin{pmatrix} 0 & 0 & 1 \\ 0 & 0 & 0 \\ 1 & 0 & 0 \end{pmatrix}$	
$\frac{1}{\sqrt{2}} \begin{pmatrix} 1 & 0 & 0 \\ 0 & -1 & 0 \\ 0 & 0 & 0 \end{pmatrix}$		$\frac{1}{\sqrt{2}} \begin{pmatrix} 1 & 0 & 0 \\ 0 & 0 & 0 \\ 0 & 0 & -1 \end{pmatrix}$	
$\frac{1}{\sqrt{6}} \begin{pmatrix} 1 & 0 & 0 \\ 0 & 1 & 0 \\ 0 & 0 & -2 \end{pmatrix}$		$\frac{1}{\sqrt{6}} \begin{pmatrix} 1 & 0 & 0 \\ 0 & -2 & 0 \\ 0 & 0 & 1 \end{pmatrix}$	
$\frac{1}{\sqrt{6}} \begin{pmatrix} -2 & 0 & 0 \\ 0 & 1 & 0 \\ 0 & 0 & 1 \end{pmatrix}$		$-\frac{1}{\sqrt{6}} \begin{pmatrix} -2 & 0 & 0 \\ 0 & 1 & 0 \\ 0 & 0 & 1 \end{pmatrix}$	

Figure 7: Select unit moment tensors and associated beachballs.

### 2.3 Sources, Green functions, normal modes & source-time function

We now link these findings to the theory of dynamic elasticity and normal modes as treated earlier.

#### Volterra's Theorem

Recall the representation theorem

$$u_n(\boldsymbol{\xi}, T + T_0) = \int_{-\infty}^{\infty} dt \int_{\Sigma} u_i(\mathbf{x}, t) \hat{\nu}_j c_{ijkl} \partial_k G_{ln}(\mathbf{x}, T - t, \boldsymbol{\xi}, T_0) d^2 \mathbf{x}, \quad (2.27)$$

stating that it suffices to know the displacement on the fault  $\mathbf{u}(\mathbf{x}, t)$  in time to determine displacement anywhere. This is an example of a *forward modeling approach*, in that one takes initial and boundary conditions to predict the displacement, or solution to the momentum equation. To use eq. (2.27), one needs to compute the Green functions  $G_{ln}$ , i.e. the response of the medium to a unidirectional force. For complicated media, numerical techniques are needed to do this. One can turn this around by assuming the source term, and derive earth structure, i.e. solve an *inverse problem*. Eq. (2.27) can be written more concisely using the above findings as

$$u_n(\mathbf{x}, t) = \int_{\Sigma} u_i(\boldsymbol{\xi}, \tau) c_{ijkl} \nu_j * \partial_k G_{ln} d^2 \boldsymbol{\xi} = \int_{\Sigma} m_{kl} * \partial_k G_{ln} d^2 \boldsymbol{\xi} = M_{kl} * G_{ln, k}, \quad (2.28)$$

where we have encapsulated the temporal convolution by “\*”, used the definition of the moment-density tensor, and denoted  $G_{np,q} := \partial_q G_{np}$ .

### Glut, faults & modes

The acceleration response of  $\oplus$  may be written in the general summation form as

$$\mathbf{a}(\mathbf{x}, t) = \sum_k (a_k \sin \omega_k t + b_k \cos \omega_k t) \mathbf{s}_k(\mathbf{x}), \quad (2.29)$$

where the coefficients are given by

$$\begin{Bmatrix} a_k \\ b_k \end{Bmatrix} = \int_{t_0}^{t_f} \overbrace{\left[ \int_{\oplus} \partial_t \mathbf{f} \cdot \mathbf{s}_k d^3 \mathbf{x} + \int_{\partial \oplus} \partial_t \mathbf{t} \cdot \mathbf{s}_k d^2 \mathbf{x} \right]}^{c_k(t)} \begin{Bmatrix} \sin \omega_k t \\ \cos \omega_k t \end{Bmatrix} dt, \quad (2.30)$$

and for a general rupture in 3D region  $\Sigma$ , the term in square brackets takes the form

$$c_k(t) = - \int_{\Sigma} (\nabla \cdot \partial_t \mathbf{S}) \cdot \mathbf{s}_k d^3 \mathbf{x} + \int_{\partial \Sigma \cap \partial \oplus} (\hat{\mathbf{n}} \cdot \partial_t \mathbf{S}) \mathbf{s}_k d^2 \mathbf{x} = \int_{\Sigma} \partial_t \mathbf{S} : \boldsymbol{\epsilon}_k d^3 \mathbf{x} + \int_{\partial \Sigma - \partial \Sigma \cap \partial \oplus} (\hat{\mathbf{n}} \cdot \partial_t \mathbf{S}) \mathbf{s}_k d^2 \mathbf{x} \quad (2.31)$$

In the case of an ideal fault, recognizing  $\mathbf{S} = \mathbf{m} \delta_{\Sigma}$ , coefficients may be written in terms of the surface moment-tensor density as

$$\begin{Bmatrix} a_k \\ b_k \end{Bmatrix} = \int_{t_0}^{t_f} \int_{\Sigma} \partial_t \mathbf{m} : \boldsymbol{\epsilon}_k(\mathbf{x}) \begin{Bmatrix} \sin \omega_k t \\ \cos \omega_k t \end{Bmatrix} d^2 \mathbf{x} dt. \quad (2.32)$$

The acceleration response in this moment-tensor framework is

$$\mathbf{a}(\mathbf{x}, t) = \sum_k \overbrace{\mathbf{M} : \boldsymbol{\epsilon}_k(\mathbf{x}_s)}^{\text{amplitude}} \overbrace{\mathbf{s}_k(\mathbf{x})}^{\text{shape}} \overbrace{\cos \omega_k(t - t_s) H(t - t_s)}^{\text{oscillations } t \geq t_s}, \quad (2.33)$$

which is linear in  $\mathbf{M}$  such that inversions for the moment tensor are “easy”.

### Source-time function

The temporal behavior of the source is modeled via the glut rate as

$$\partial_t \mathbf{S} = \dot{\mathbf{M}} \delta(\mathbf{x} - \mathbf{x}_s), \quad (2.34)$$

where  $\dot{\mathbf{M}}(t) = \int_{\Sigma} \partial_t \mathbf{S} d^2 \mathbf{x}$  is the *moment-rate tensor*. Assuming that the source is synchronous in all components of  $\mathbf{M}$ , one also writes

$$\dot{\mathbf{M}}(t) = \sqrt{2} M_0 \hat{\mathbf{M}} \dot{m}(t), \quad (2.35)$$

where the normalized source-time function  $\dot{m}(t)$  satisfies

$$\int_{t_0}^{t_f} \dot{m}(t) dt = 1. \quad (2.36)$$

For a planar fault with non-deviatoric initial stress it takes the weighted-average form of the slip speed

$$\dot{m}(t) = \frac{1}{M_0} \int_{\Sigma} \mu \partial_t \Delta s \, d^2 \mathbf{x}. \quad (2.37)$$

Source-time functions are often approximated as a sequence of box-cars, trapezoids, isosceles triangles, or Gaussians.

### Analytical solutions: Point source in a homogeneous whole space

We now turn to examining the resultant propagation effects due to different earthquake types. In an elastic homogeneous whole space, the far-field compressional-wave displacement upon a moment-tensor source at  $r = 0$  in polar coordinates  $(r, \theta, \phi)$  takes the analytical form (Aki and Richards, 2002)

$$u_r = \frac{1}{4\pi\rho v_p^3 r} \dot{M}(t - r/v_p) \sin 2\theta \cos \phi. \quad (2.38)$$

The first term is an amplitude, note the cubic dependence on the velocity, and decays inversely linear with distance. The second term represents a temporal pulse propagating at speed  $v_p$ , i.e. the *source time function*. The trigonometric terms describe the radiation pattern, in this case 4 lobes with each 2 positive and negative lobes. The shear-wave displacements perpendicular to  $u_r$  take the form

$$u_\theta = \frac{1}{4\pi\rho v_s^3 r} \dot{M}(t - r/v_s) \cos 2\theta \cos \phi, \text{ and} \quad (2.39)$$

$$u_\phi = \frac{1}{4\pi\rho v_s^3 r} \dot{M}(t - r/v_s) (-\cos \theta \sin \phi). \quad (2.40)$$

This  $S$ -wave motion does not have nodal planes, and thus does not reflect the fault geometry as clearly as  $P$ -waves. It is noteworthy to examine the average amplitudes between  $P$  and  $S$  waves which depends on  $(v_p/v_s)^3 \approx 5$ , suggesting that  $S$  waves typically have much larger amplitudes than  $P$  waves.

## 2.4 Seismic sources in the real world

### Fault classification

Most earthquake process studies deal with *transform faults* (e.g. San Andreas, Anatolian fault), and to a lesser degree with subduction zones (e.g. Japan, Chile), although deep subduction quakes are the strongest events ever recorded (Chile 1960,  $Mw = 9.5$ , Alaska 1964  $Mw = 9.2$ , Sumatra 2004  $Mw = 9.1$ ) and trigger the vast majority of cumulative seismic energy. This may have several reasons, amongst which are historical (large populations along faults, many subduction zones are off-shore especially around the Pacific), their associated risk (faults are shallow, hence destructive surface waves prominent), and physical in that the stress field and rock mechanics around faults are more accessible and the origin of deep subduction seismicity still controversially debated.

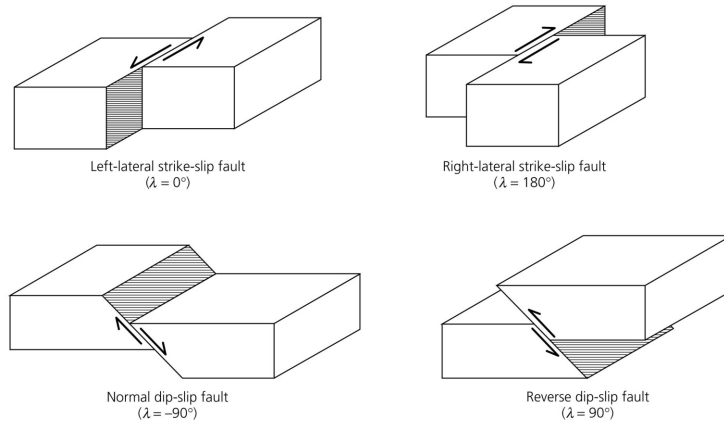
**Figure 4.2-3: Basic types of faulting.**

Figure 8: *Basic types of faulting. Top: transform type (e.g. San Andreas). Bottom: subduction type (e.g. Chile). Reverse and thrust faulting is the same.*

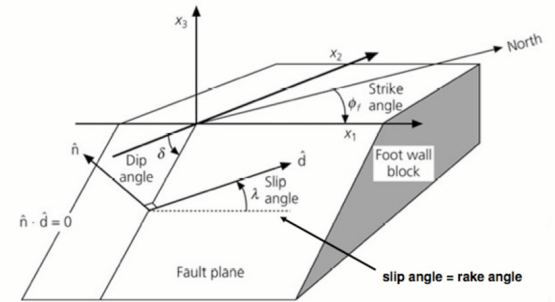
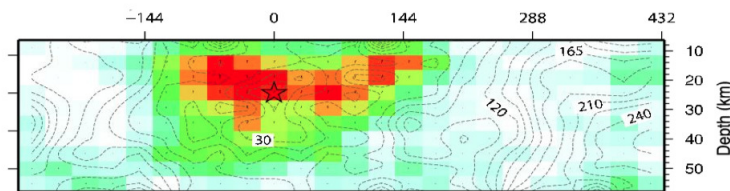


Figure 9: *Definition of fault geometry. The fault plane separates the lower "foot wall" from the upper "hanging wall". Angles are defined such that the dip angle is less than  $90^\circ$ , strike is measured from North. Note: Slip angle=rake angle.*

A M9 event releases much more energy - 20 '000 more - than a M6.3 event. This depends on the size of the fault and the amount of slip.

Christchurch: M6.3, slip 1m, source area 30\*10km



Tohoku: M9, slip up to 18m, source area 300\*40km

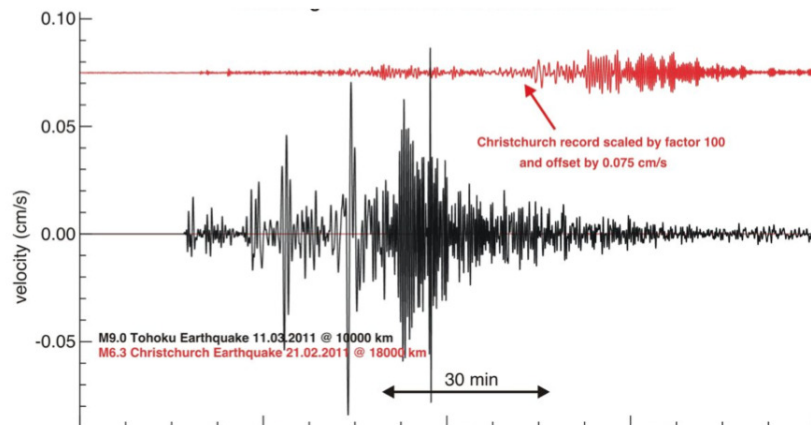


Figure 10: *Comparison of M6.3 Christchurch (Feb 21, 2011) and M9.0 Tohoku (Mar 11, 2011) events. Top: Kinematic source models at the same scale. Bottom: Ground velocity for both events recorded in Zurich.*

## Kinematic & dynamic rupture

While the point-source approximation along with the determination of earthquake parameters using moment tensors has its well-defined realm of validity and works surprisingly well, clearly the finite extent of earthquake rupture needs to be taken into account for a general characterization of earthquakes. We distinguish *kinematic* and *dynamic* processes, where the former assumes a given slip distribution and describes waves emanate from the ruptured region, whereas the latter deals with the foundations of time-dependent evolution, actual cause and nature of slip across the fault. We keep this treatise at a qualitative minimum, as these subjects easily fill their own course and most global, structural seismologists tend to rely on point-source approximations.

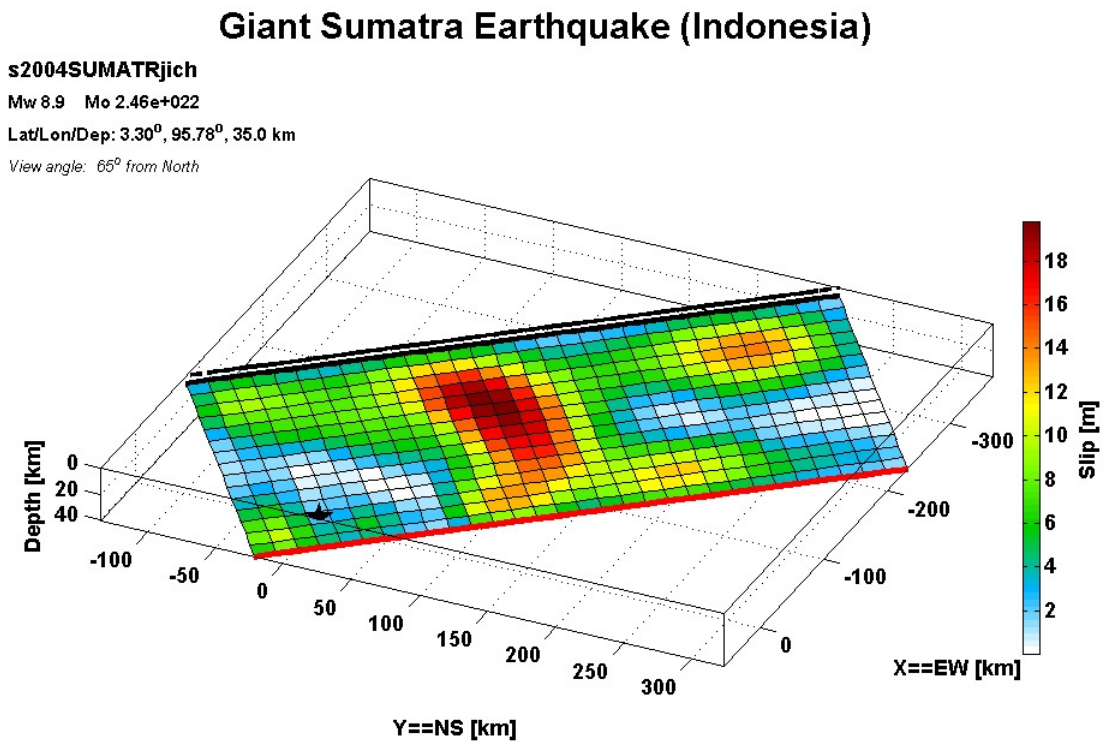


Figure 11: *Kinematic source model for the giant Sumatra earthquake on December 26, 2004.  $M_w = 8.9$ , length: 450km, width: 180km, rise time: 999 seconds, rupture speed: 2km/s.*

**Kinematic source** models are usually obtained by seismic waveform modeling, i.e. by inverting near-field (strong-motion), regional-distance, and/or far-field (teleseismic) seismograms. For seismic-hazard studies, kinematic models are often “simply” simulated. Haskell (1964) uses a simple ramp function to represent slip on a fault as shown in Figure 11, where  $D$  is the final slip. Thus, the source can be characterized by 1) The fault length  $L$ , 2) the fault width  $W$ , 3) Rupture velocity  $V_r$ , 4) Permanent slip  $D$  and 5) Rise time.

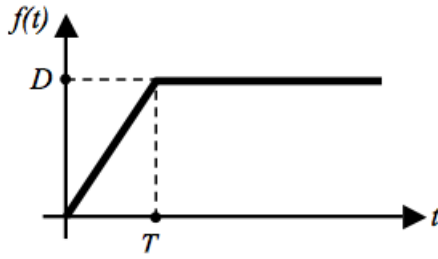


Figure 12: *Ramp function describing the kinematic source model after Haskell.*

**Dynamic ruptures** characterize the earthquake process based on the material properties around the source volume and the initial and boundary conditions for the forces and stresses acting on the fault plane. The slip-rate vector is obtained by solving the elasto-dynamic equations of motion under the assumption of some constitutive law. Dynamic rupture models are usually obtained from an existing kinematic model by an inversion/modeling approach, but not from waveforms directly, or for simulated initial conditions/stress distributions. Dynamic rupture can be described as a two-step process: (1) formation of a crack and (2) propagation or growth of the crack. The crack tip serves as a stress concentrator due to a driving force (that could be the tectonic loading); if the stress at the crack tip exceeds some critical value (material strength), then the crack grows unstably accompanied by a sudden slip and stress drop. Once a fault has been formed its further motion is controlled by friction sliding, which is a contact property.

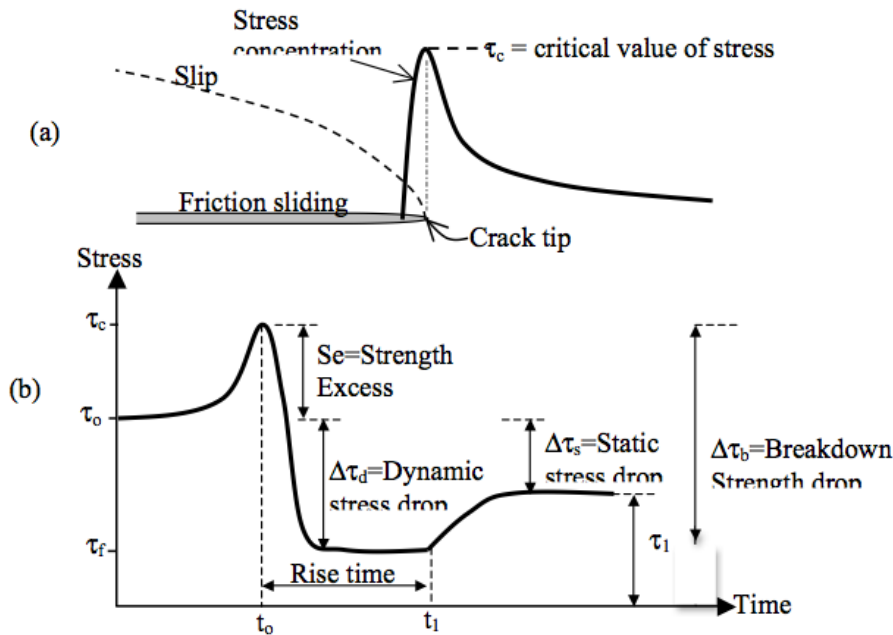


Figure 13: *a) Idealized model of a crack rupture with stress concentration in the crack tip and slip in the friction sliding zone. (b) Stress time evolution at a point on the crack in which the fault begins to slip at  $t_0$  and stop at time  $t_1$ .  $\tau_c$  is the critical stress or yielding stress,  $\tau_0$  is the initial stress,  $\tau_f$  dynamic frictional value,  $\tau_1$  final stress after the slip has stopped.*

## Scaling relations: Earthquake magnitudes, recurrence

**The power of Power laws:** The number of cities having a certain population size is found to vary as a power of the size of the population. Power laws also govern phenomena such as frequencies of words in most languages, frequencies of family names, sizes of craters on the moon and of solar flares, the sizes of power outages, and wars, the popularity of books and music.

Many natural phenomena follow (somewhat surprisingly) power laws which describe the logarithmic relationship between, for instance, frequency of occurrence and size of the event as quasi-linear. The classic plot relates the magnitude of earthquakes to the size of the rupture, following the empirical relationship  $M_0 \sim A^{3/2}$ . This concept is closely related to *self-similarity*, stating that small and large earthquakes are statistically identical, and their properties differ merely by a scaling factor.

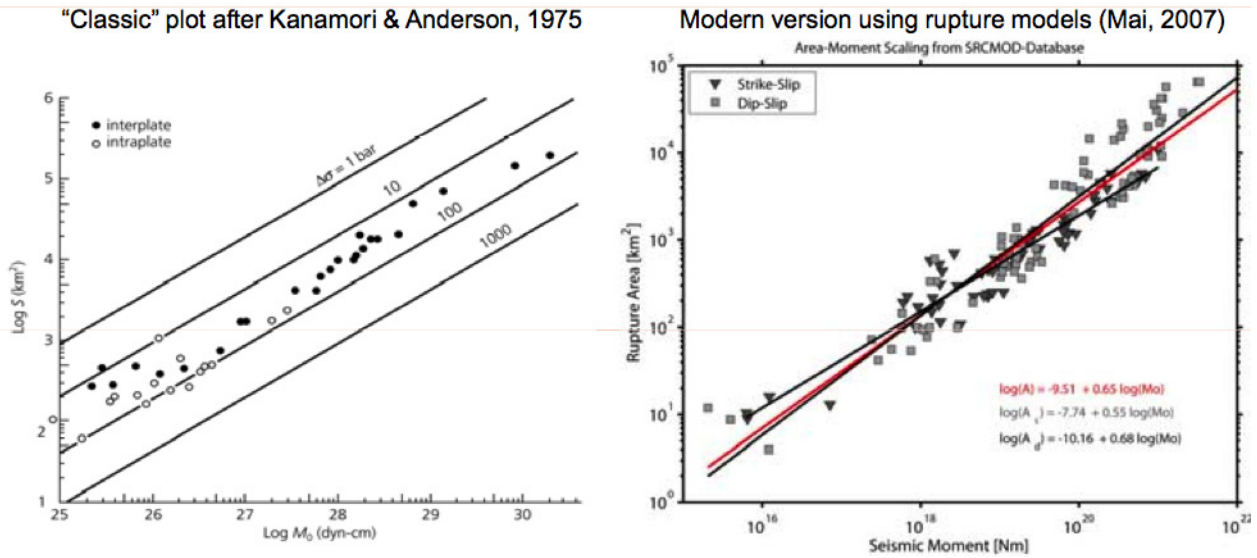


Figure 14: *Scaling relation between magnitude and size of slip area. Note that the relation is valid for inter- and intraplate, subduction and transform fault events.*

While not really a scaling law, it is important to distinguish different measures of the magnitude: Magnitude measurements using body and surface waves saturate, such that they do not properly estimate the size of large earthquakes at low frequencies. This is especially crucial for Tsunami warnings. The *moment magnitude*  $M_w$  [N m] introduced by Hiroo Kanamori is the current standard to characterize very large events via

$$M_w = \frac{2}{3} (\log_{10} M_0 - 9.1) \quad (2.41)$$

where  $M_0$  is the scalar moment measured in [N m]<sup>1</sup>.

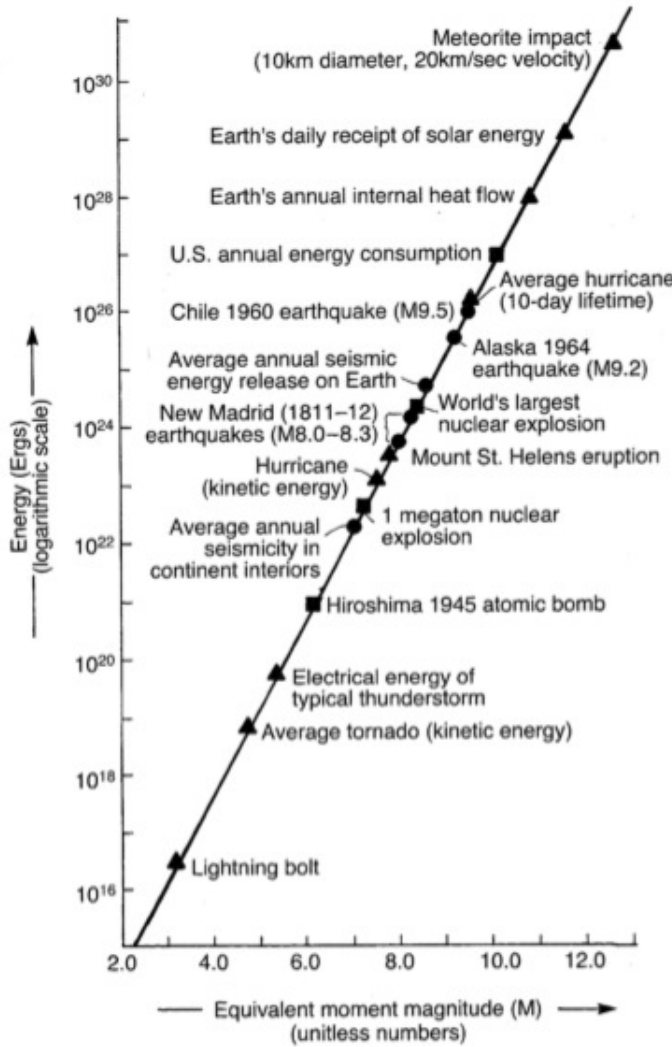
<sup>1</sup>the original Hanks & Kanamori paper defined moment magnitude as  $2/3 \log M_0 - 10.7$  (dyne-cm), however, Aki & Richards use  $\log M_0 = 1.5M_w + 16.1$ . Here we use the Aki & Richards definition of  $M_w$ .



*Example:* The seismic moment of the *largest possible earthquake* for a given fault length  $L$  (Antarctica to Alaska: 15,000km) is

$$M_0^{\max} = \mu \bar{u} L Z_{\max} / \sin \delta, \quad (2.42)$$

$\mu$ : shear modulus ( $\approx 1.3 \cdot 10^9 \text{ dyn/cm}^2$ ),  $\bar{u}$ : average slip ( $\approx 2.5 \cdot 10^{-5} L$ ),  $Z_{\max}$ : maximal slip depth ( $\approx 70 \text{ km}$ ),  $\delta$ , dip angle ( $\approx 10$ ), such that we obtain an upper limit of  $M_w < 10.5$ .



**Figure 3.25** Equivalent moment magnitude of a variety of seismic (dots), human-made (squares), and other phenomena (triangles).

Source: A. C. Johnston, "An earthquake strength scale for the media and the public" in *Earthquakes and Volcanoes 22* (no. 5): 214-16. U.S. Geological Survey.

Figure 15: *Moment magnitude and energy release from lightning to meteorites. Note the logarithmic scales.*

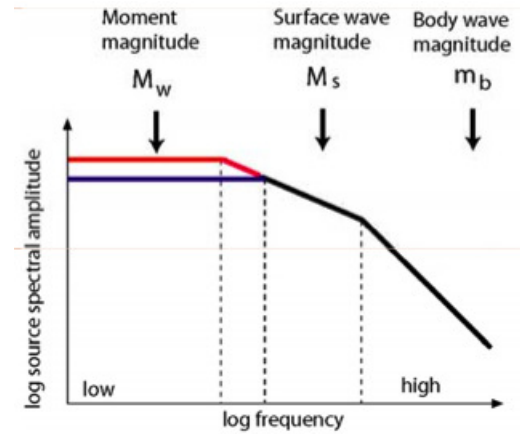
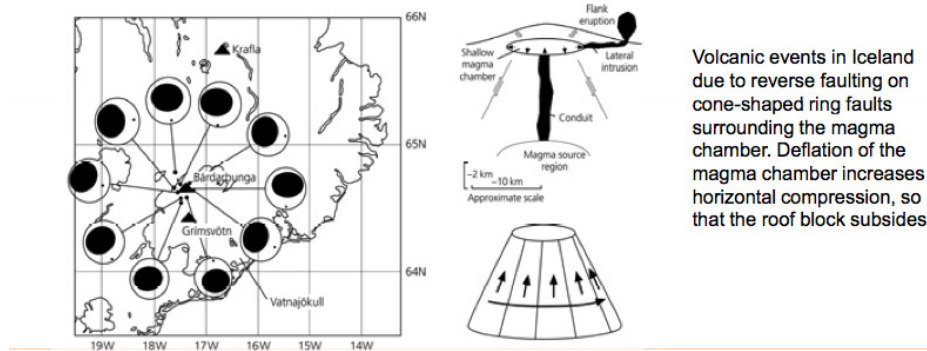


Figure 16: *Body and surface wave magnitudes saturate once earthquakes exceed a certain size because added energy release in very large earthquakes is at periods  $> 20\text{s}$ . Body and surface wave magnitudes do not exceed 6.5 and 8.4, respectively.*

### Tremors, volcanoes, glaciers, meteorites, nuclear monitoring

An extensive variety of natural, earth-based, external, or man-made events exists that trigger seismic motion that can be recorded at teleseismic distances using conventional seismometers: large/fast glacial motions (M5.1), extraterrestrial impacts (Tunguska, Russia 1908: ~M5), nuclear tests (up to M5), volcanic magma chambers (>M5), slow-slip (tremor) events in subduction zones (energy release over days/weeks up to M6.7), or ambient “noise” generated in the oceans. Reverse faulting in Iceland causes seismic events, resulting in deflation and *compensated linear vector dipole* moment tensor (CLVD).

### CLVD type focal mechanism



- Model of an inflating magma dike: crack opening under tension.

$$\mathbf{M} = \begin{pmatrix} \lambda & 0 & 0 \\ 0 & \lambda & 0 \\ 0 & 0 & \lambda + 2\mu \end{pmatrix} = \begin{pmatrix} E & 0 & 0 \\ 0 & E & 0 \\ 0 & 0 & E \end{pmatrix} + \begin{pmatrix} -2/3\mu & 0 & 0 \\ 0 & -2/3\mu & 0 \\ 0 & 0 & 4/3\mu \end{pmatrix}$$

Isotropic tensor                      CLVD component

Figure 17: *Fried-egg events in Iceland: simultaneous vertical extension and horizontal compression.*

## Further reading

- Aki, K., and P. G. Richards, *Quantitative Seismology*, 2nd Edition, University Science Books, 2002: chapters 3, 10,11.
- Backus, G. and M. Mulcahy, 1976a. *Moment tensors and other phenomenological descriptions of seismic sources – 1. Continuous displacements*, Geophys. J. Roy. Astr. Soc., 46, 341-361.
- Burridge, R. and L. Knopoff, 1964. *Body force equivalents for seismic dislocations*, Bull. Seism. Soc. Am. 54, 1875-1888.
- Dahlen, F. A., and J. Tromp, 1998. *Theoretical Global Seismology*, Princeton University Press.
- Stein, S. and M. Wysession, 2003. *An Introduction to Seismology, Earthquakes, and Earth Structure*, Blackwell Publishing, chapter 4.
- Takei, Y. and Kumazawa, M., 2007. *Why have the single force and torque been excluded from seismic source models?* Geophys. J Int., 118, 1, 20 - 30.
- Other resources:  
CMT solutions: [globalcmt.org](http://globalcmt.org)  
Southern California Earthquake Center: [scec.org](http://scec.org)  
USGS Earthquakes: [earthquake.usgs.gov](http://earthquake.usgs.gov)  
Saudi Geological Service: [sgs.org.sa](http://sgs.org.sa)  
Incorporated Research Institutions for Seismology (IRIS): [www.iris.edu](http://www.iris.edu)  
Exotic seismic events: [ds.iris.edu/spud/esec](http://ds.iris.edu/spud/esec)

**Disclaimer:** These notes have been blatantly assembled using text books (Dahlen & Tromp, Stein & Wysession), and other course notes (Tony Dahlen, Martin Käser, Martin Mai, Heiner Igel). If there is such a thing as “copyright” on these notes, it would be merely claimed to Tarje Nissen-Meyer and Daniel Peter based on the actual editing efforts and assembly thoughts on how to organize these various topics together into one coherent (?) flow.